Contiuous Spectral Volume Rendering

Alen Kurtagić, Matija Marolt, Žiga Lesar, Ciril Bohak

University of Ljubljana, Faculty of Computer and Information Science E-mail: ak84795@student.uni-lj.si, {matija.marolt, ziga.lesar, ciril.bohak}@fri.uni-lj.si

Abstract

Path tracing applications often overlook wave optics and wavelength dependency effects, impacting the accuracy of visual representations. This paper presents the integration of continuous spectral rendering support into the web-based volumetric path tracing framework to simulate wave optics effects. Spectral rendering, which accounts for wavelength-specific photon behavior, enhances scene realism by providing a more accurate depiction of light interaction with materials. We developed a spectral volume renderer, leveraging WebGL and Python for implementation and validation. Key wavelength-dependent phenomena, such as Rayleigh scattering, fluorescence, and metamerism, are simulated, demonstrating the renderer's capability to produce realistic visual effects. The implementation involves enhancing the Monte-Carlo path tracing algorithm with spectral characteristics and using Gaussian approximations of CIE 1931 color matching functions for accurate color transformations.

1 Introduction

Light, a fundamental aspect of our perception of the world, exhibits both wave and particle characteristics. It can be simulated with photons of different wavelengths constituting a spectrum of colors. The spectral nature of light, encompassing its wavelength-dependent behavior, is crucial for accurately representing various optical phenomena such as Rayleigh scattering [5], metamerism [4], and even fluorescence[14]. Traditional rendering techniques often simplify the behavior of light by modeling it as a triplet of wavelengths (RGB) [10], leading to approximations that may not capture the full complexity of realworld scenes. In this paper, we tackle the problem of simulating wavelength-dependent optical phenomena in volumes, also known as spectral volume rendering. In biomedical imaging, spectral volume rendering can enhance the visualization of tissues and structures by accurately depicting how different wavelengths interact with biological materials. In the field of astronomy, it can simulate the appearance of celestial objects by accounting for the wavelength-dependent scattering and absorption of light in various media. Spectral volume rendering is valuable in creating realistic visual effects in computer graphics, such as simulating the atmospheric scattering that causes the sky to appear blue or the sunsets to be red.

It also has applications in cultural heritage preservation, where accurate color reproduction is essential for documenting and restoring artworks and historical artifacts.

2 Related Work

Spectral volume rendering has been a topic of interest for several decades due to its ability to represent the interaction of light with different materials accurately. One of the foundational works in this field was presented by Noordmans et al. [9], who explored spectral volume rendering techniques and their applications in accurately visualizing volumetric data by considering the spectral properties of light and its interaction with matter. Building on this foundation, Bergner et al. [3] introduced an interactive spectral volume rendering approach, which allowed for real-time manipulation and exploration of volumetric datasets and supports real-time re-lighting of the scene. The authors introduce a post-illumination technique to generate new spectral images for arbitrary light colors. The follow-up work by Bergner et al. [4] presents a lowdimensional subspace method used to act as the spectral information carrier at low overhead. The method's performance is adequate for generating spectral images in real time for arbitrary light spectra under a fixed viewpoint.

Abdul-Rahman and Chen [1] proposed a spectral volume rendering technique based on the Kubelka-Munk theory of diffuse reflectance. The method suits spectral volume rendering for participating media and solid objects. Moreover, the optical effects are more accurately represented than in the traditional RGB accumulation raycasting approach. Strengert et al. [11] developed a GPUbased raycasting technique for spectral volume rendering also based on Kubelka-Munck theory. Their implementation supports several spectral optical effects, such as selective absorption and dispersion in refractive materials, and enables interactive performance of moderately-sized datasets.

There are many volume rendering frameworks developed for different platforms (e.g., Inviwo [6], Paraview [2], Volumetric Path Tracing (VPT) [8]). For broader accessibility, we decided to implement our approach in a webbased volumetric path tracing framework VPT [8], which allows simple extension with new volumetric rendering techniques.

3 Background

It is essential to understand the basic transformation of photon wavelength into perceived colors for the implementation of a realistic light simulation in rendering.

Visible light is a segment of the broader electromagnetic spectrum. Human perception of light is limited to electromagnetic radiation [10], with wavelengths ranging from approximately 380 nm (perceived as blue) to 700 nm (perceived as red). This range encompasses our whole visible spectrum, and radiometric measurements within this bandwidth are crucial for accurately simulating how light interacts with objects and how it is perceived as different colors. Light sources are characterized by their Spectral Power Distribution (SPD), which describes the intensity of light they emit at different wavelengths. An example of an SPD is a standard D65 daylight outlined by the left line chart in fig. 1, demonstrating the distribution of emitted light across the visible spectrum.

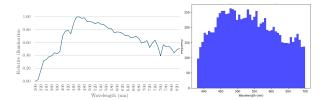


Figure 1: D65 daylight spectral power distribution (left) and the histogram of 10,000 samples drawn from it (right).

Similarly to light sources, the optical properties of materials are defined using wavelength-dependent functions such as reflectance, absorption, and transmission. These functions describe how a material interacts with light across different wavelengths, influencing the material's appearance under various lighting conditions.

The tri-stimulus response of the human eye to a light spectrum forms the biological basis for the RGB (Red, Green, Blue) color model [10], which is utilized by various technologies, such as display screens. However, this model has limitations because it can only represent a subset of colors visible to the human eye, known as the RGB color space. The sRGB color space, a standard for RGB color models, also includes gamma correction to adjust for the non-linear response of human vision, allocating more bits to darker colors. The XYZ color space was introduced by the International Commission on Illumination (CIE) as part of an effort to create a color model that would encompass the full range of human color vision. Unlike RGB, XYZ is derived from a series of experiments that measured human visual response to different light wavelengths. This led to the creation of the XYZ color-matching functions. These functions are mathematical representations of the average human eye's color sensitivity across the visible spectrum and are pivotal in accurately transforming light wavelengths into perceived colors.

Understanding the phenomena associated with light as a spectrum is crucial, as we will simulate the following phenomena in our implementation.

Rayleigh Scattering [5] explains why the sky is blue and why sunsets often appear red. As sunlight passes through the Earth's atmosphere, light of shorter wavelengths (such as blue) scatters more widely in random directions, while longer wavelengths (such as red) scatter less and remain more concentrated in the direction of the light source. This differential scattering is due to the size of the atmospheric particles being smaller than the wavelength of visible light, affecting shorter wavelengths more significantly. During the day, the sky appears blue because blue light is scattered across the sky. At sunset, the sunlight must pass through a greater thickness of the atmosphere, scattering more blue light out of the direct path to our eyes and allowing more red light to reach us directly, hence the reddish hues.

Fluorescence [14] occurs when materials absorb light at one wavelength, usually ultraviolet, and emit light at a longer, visible wavelength. This process involves the absorption of light energy, which excites electrons to a higher energy state. When these electrons return to their original energy state, they emit photons at a longer wavelength than the light absorbed. This phenomenon is widely observed in various materials and biological entities, providing distinct visual effects that are particularly pronounced under UV light.

Metamerism [4] is a phenomenon that arises from the complex interactions between the spectral properties of light and human visual perception. This effect occurs when two objects, each possessing distinct spectral reflectance characteristics, appear identical in color under certain SPD of the light source illuminating these objects. Despite their inherent differences in how they reflect light, the specific SPD can cause both objects to reflect wavelengths that are processed similarly by the human eye, resulting in the perception of the same color.

4 Method

Our renderer enhances the existing Monte-Carlo path tracing algorithm used in VPT [8] by incorporating spectral characteristics into the simulation. Each photon in our renderer is assigned a specific wavelength. Building upon the Monte-Carlo path tracing foundation provided by VPT, our spectral renderer assigns each photon a wavelength. This addition allows photons to exhibit wavelength-dependent behavior as they traverse the volume, such as varying degrees of absorption, reflection, and scattering, which are all defined with certain custom functions.

4.1 Wavelength sampling techniques

To effectively simulate the spectrum of visible light, photons must be assigned wavelengths that reflect this range. We utilize a function named sampleWavelength for uniform sampling across this spectrum. However, to mimic real-world light conditions more accurately, we consider the SPD of natural daylight, specifically D65. The function sampleWavelengthD65 employs rejection sampling to select wavelengths according to the D65 SPD, ensuring that the distribution of photon wavelengths accurately represents natural lighting conditions. The histogram in Figure 1 illustrates the results of sampling the D65 SPD in our renderer.

In addition to visible light, it is crucial to consider ultraviolet (UV) photons for materials exhibiting fluorescence. These materials absorb UV light and re-emit it at longer, visible wavelengths. To simulate this, the sampleWavelengthUV function extends the wavelength 5 sampling below 380 nm to include UV wavelengths, crucial for rendering fluorescent effects. It is important to note that direct sampling from a single SPD corresponds to simulating just one light source. To facilitate the simulation of multiple light sources, we propose aggregating the SPDs of all relevant light sources into a composite SPD. This composite can then be sampled to reflect the combined influence of all light sources. Importantly, when a wavelength sampled from this composite SPD directly interacts with a light source, we apply rejection sampling to this specific interaction.

4.2 Gaussian approximations of color matching functions

To convert the wavelength of a photon into the XYZ color space, we utilize the CIE 1931 color matching functions. For simplicity, we have chosen to approximate these functions using Gaussian functions. This approach follows the findings of Wyman et al. [13], who identified optimal Gaussian approximations for \tilde{x} , \tilde{y} and \tilde{z} that closely mimic the original x, y, and z functions which resemble closely the standard CIE 1931 color matching functions.

4.3 The color pipeline: wavelength to sRGB

Converting a photon's wavelength into a perceivable color involves several steps. Initially, we calculate the XYZ color space values corresponding to the given wavelength using the Gaussian approximated CIE 1931 color matching functions. Subsequently, these XYZ values are transformed into the linear RGB color space through a linear matrix transformation [10]. For correct color reproduction on a physical display, gamma correction must be applied after the Monte-Carlo integration. This step is handled by the VPT tone mapping.

4.4 Implementation

The VPT framework utilizes transfer functions to map the voxel value to a density and RGB albedo. However, with the introduction of wavelength dependency, it is also necessary to adjust the material representation. We now define albedo using a 3D function that varies in both density and wavelength, a method that mirrors our shift from RGB colors in environment maps to SPD for light sources. For instance, a material can be configured to exhibit high albedo at longer wavelengths and low albedo at shorter wavelengths, producing colors with a more reddish hue. Additionally, we have implemented control over the scattering direction of photons through the anisotropy pa-

rameter of the Henyey-Greenstein phase function [12]. This parameter is controlled by a 2D function that relates a wavelength to the anisotropy parameter. For example, by assigning a high anisotropy value to longer wavelengths, photons at these wavelengths scatter predominantly around the incident direction. Conversely, assigning a low anisotropy value to shorter wavelengths causes these photons to scatter more diffusely. This entire configuration is designed to emulate the Rayleigh scattering observed in the Earth's atmosphere.

5 Results

We demonstrate the capabilities of our spectral renderer by visualizing the three phenomena.

Rayleigh scattering: Our first simulation depicts Rayleigh scattering. To achieve this, we adjusted our methods to control the scattering of different wavelengths effectively. We opted not to use the SPD of a D65 daylight source for the light source simulation, as it already represents sunlight after atmospheric interaction, rather than the sun itself. In our experiment, we simulated sunlight by uniformly sampling all wavelengths across the visible spectrum. We set the albedo for all wavelengths at 0.8, ensuring that most wavelengths predominantly scatter rather than absorb. The anisotropy settings were adjusted to vary with wavelength; the shortest visible wavelengths were set to an anisotropy of zero, increasing to one for the longest wavelengths. This gradation in anisotropy helps to simulate the characteristic blue of the sky and the reddish colors directly behind the sun (light source). The leftmost image in fig. 2 illustrates the effects of Rayleigh scattering under these settings. The light does not appear completely white, as the SPD is sampled uniformly.

Flouroscence: Next, we depict fluorescence. We achieved this by making the light source's SPD only emit low wavelengths, more specifically from 275 nm to 450 nm, which encompasses UV lights as well as blue and purple visible light. We then transformed UV wavelengths (lower than 380 nm) into longer wavelengths using a Gaussian distribution with a peak at 550 nm. This gives the effect of the material being a different color than the light, as it is emitting its own light. The fact that the light source only contains blue and purple wavelengths and the material appears greenish instead of matching the hue of the light source demonstrates the presence of fluorescence. If the material did not fluoresce, it would be expected to appear similar to the blue and purple hues of the light source. The second image from the left in fig. 2 shows a fluorescent frog.

Metamerism: The final phenomena we want to present in the adapted VPT framework is metamerism. We achieved this on a very simplified example. One material scatters only the low end of the spectrum, while the other scatters the low and also the high end. If we sample light with D65 distribution, which contains all visible wavelengths, the two materials will scatter and absorb different wavelengths, thus appearing in different colors. How-

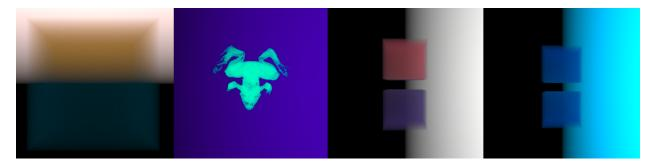


Figure 2: From left to right: Rayleigh scattering, fluorescence, and metamerism demonstrated by using two different illuminants.

ever, if we sample only one-half of the D65 SPD, the two materials will scatter the same wavelengths, thus appearing the same color under that lighting. The third image from left to right in fig. 2 shows two cubes being different colors under D65 SPD lighting, while the rightmost image in fig. 2 shows them being the same color, as we only light the lower half of the D65 SPD.

Our implementation is available on GitHub [7].

6 Conclusion

In this work we implemented spectral volumetric rendering into an existing web-based volumetric path tracing framework. We support continuous spectra and transfer functions and demonstrate the results of our implementation through the visualization of various phenomena: Rayleigh scattering, which elucidates why the sky appears blue; fluorescence, which reveals vivid colors in materials under specific lighting conditions; and metamerism, which changes our perceptions of color under varying light sources. These examples underscore the accuracy of our spectral volume renderer. The benefits of supporting spectral effects results in slower rendering times. Looking ahead, there are several possibilities for enhancing our implementation. Adding support for multiple light sources with a combined SPD would allow for more dynamic and realistic lighting simulations. Further, the current static coding of material behaviors—such as fluorescence, variable albedos based on wavelength and density, and the SPDs themselves-could be made dynamic through user interface enhancements, enabling users to adjust these parameters interactively based on their needs.

Acknowlegment

This research was conducted as part of the basic research project *Cell visualization of unified microscopic data and procedurally generated sub-cellular structures* [project number J2-50221], funded by the Slovenian Research and Innovation Agency (Javna agencija za znanstvenoraziskovalno in inovacijsko dejavnost RS) from the state budget.

References

 Alfie Abdul-Rahman and Min Chen. Spectral volume rendering based on the kubelka-munk theory. *Computer Graphics Forum*, 24(3):413–422, 2005.

- [2] James Ahrens, Berk Geveci, and Charles Law. ParaView: An end-user tool for large data visualization. In *Visualization Handbook*. Elesvier, 2005. ISBN 978-0123875822.
- [3] S. Bergner, T. Moller, M.S. Drew, and G.D. Finlayson. Interactive spectral volume rendering. In *IEEE Visualization*, 2002. VIS 2002., pages 101–108, 2002.
- [4] S. Bergner, T. Moller, M. Tory, and M.S. Drew. A practical approach to spectral volume rendering. *IEEE Transactions on Visualization and Computer Graphics*, 11(2):207–216, 2005.
- [5] Hendrik Christoffel Hulst and Hendrik C van de Hulst. Light scattering by small particles. 1981.
- [6] Daniel Jönsson, Peter Steneteg, Erik Sundén, Rickard Englund, Sathish Kottravel, Martin Falk, Anders Ynnerman, Ingrid Hotz, and Timo Ropinski. Inviwo - a visualization system with usage abstraction levels. *IEEE TVCG*, 26(11):3241–3254, 2019.
- [7] Alen Kurtagić, Matija Marolt, Žiga Lesar, and Ciril Bohak. Continuous Spectral Volume Rendering. https://github.com/UL-FRI-LGM/ continuous-spectral-volume-rendering/ tree/main. [Online; accessed 5-July-2024].
- [8] Žiga Lesar, Ciril Bohak, and Matija Marolt. Real-time interactive platform-agnostic volumetric path tracing in webgl 2.0. In *Proceedings of the 23rd International ACM Conference on 3D Web Technology*, New York, NY, USA, 2018. Association for Computing Machinery.
- [9] H.J. Noordmans, H.T.M. van der Voort, and A.W.M. Smeulders. Spectral volume rendering. *IEEE Transactions on Visualization and Computer Graphics*, 6(3):196– 207, 2000.
- [10] Matt Pharr, Jakob Wenzel, and Greg Humphreys. *Physically based rendering: From theory to implementation*. The MIT Press, 4 edition, 2023.
- [11] Magnus Strengert, Thomas Klein, Ralf Botchen, Simon Stegmaier, Min Chen, and Thomas Ertl. Spectral volume rendering using gpu-based raycasting. *The Visual Computer*, 22:550–561, 2006.
- [12] Dominique Toublanc. Henyey–greenstein and mie phase functions in monte carlo radiative transfer computations. *Applied Optics*, 35:3270, 6 1996.
- [13] Chris Wyman, Peter-Pike Sloan, and Peter Shirley. Simple analytic approximations to the cie xyz color matching functions. J. Comput. Graph. Tech, 2(2):11, 2013.
- [14] Wataru Yamamoto, Bisser Raytchev, Toru Tamaki, and Kazufumi Kaneda. Spectral rendering of fluorescence using importance sampling. In SIGGRAPH Asia 2018 Posters, 2018.